# Ricolinostat enhances adavosertib-induced mitotic catastrophe in TP53-mutated head and neck squamous cell carcinoma cells

KEITARO MIYAKE[1], NAOHARU TAKANO[2], HIROMI KAZAMA[2], HIROYUKI KIKUCHI[3], MASAKI HIRAMOTO[2], KIYOAKI TSUKAHARA[1] and KEISUKE MIYAZAWA[2]

[1]Department of Otorhinolaryngology, Head and Neck Surgery, Tokyo Medical University Hospital, Shinjuku-ku, Tokyo 160-0023; Departments of [2]Biochemistry, [3]Preventive Medicine and Public Health, Tokyo Medical University, Shinjuku-ku, Tokyo 160-8402, Japan

Received August 19, 2021; Accepted March 10, 2022

DOI: 10.3892/ijo.2022.5344

**Abstract.** *TP53* mutation is one of the most frequent gene mutations in head and neck squamous cell carcinoma (HNSCC) and could be a potential therapeutic target. Recently, the WEE1 G2 checkpoint kinase (WEE1) inhibitor adavosertib (Adv) has attracted attention because of its selective cytotoxicity against *TP53*-mutated cells and has shown promising activity in early phase clinical trials. In the present study, it was demonstrated that combined treatment with Adv and a selective histone deacetylase 6 (HDAC6) inhibitor, ricolinostat (RCS), synergistically enhanced cell death induction in four out of five HNSCC cell lines with *TP53* mutation (CAL27, SAS, HSC-3, and OSC-19), one HNSCC cell line with impaired TP53 function by HPV-infection (UPCI-SCC154), and *TP53*-knockout human lung cancer cell line (A549 TP53-KO), but not in *TP53* wild-type A549 cells. Time-lapse imaging showed that RCS enhanced the Adv-induced mitotic catastrophe. Consistent with this, RCS treatment suppressed checkpoint kinase 1 (Chk1) (Ser345) phosphorylation and co-administration of RCS with Adv suppressed cyclin-dependent kinase 1 (Tyr15) phosphorylation along with increased expression of γ-H2A.X, a marker of DNA double-strand breaks in CAL27 cells. These data showed that RCS enhanced Adv-induced premature mitotic entry and cell death induction in the mitotic phase. However, although HDAC6 knockdown enhanced Adv-induced cell death with γ-H2A.X elevation, HDAC6 knockdown did not repress Chk1 phosphorylation in CAL27 cells. Our data demonstrated that the co-administration of RCS with Adv in HNSCC cells resulted in the suppression of Chk1 activity, leading to synergistically enhanced apoptosis via mitotic catastrophe in a p53-dependent manner. This enhanced cell death appeared to be partially mediated by the inhibition of HDAC6 activity by RCS.

*Correspondence to:* Dr Naoharu Takano, Department of Biochemistry, Tokyo Medical University, 6-1-1 Shinjuku, Shinjuku-ku, Tokyo 160-8402, Japan
E-mail: ntakano@tokyo-med.ac.jp

*Key words:* mitotic catastrophe, p53, head and neck squamous cell carcinoma, adavosertib, ricolinostat

## Introduction

Head and neck squamous cell carcinoma (HNSCC) is the sixth most common cancer in the world with approximately 800,000 cases being diagnosed every year (1). Advanced HNSCC shows poor prognosis and resistance to standard therapy consisting of cisplatin. Because 60-80% of HNSCC cases carry a *TP53* mutation (2-4) and human papillomavirus (HPV)-positive HNSCC shows impaired p53 function (5), therapeutic targeting of the *TP53* mutation has become a focus of research. Additionally, as p53 is functional in normal somatic cells, targeted therapy against *TP53* mutations can relieve adverse effects. Thus, owing to its selective cytotoxicity against *TP53*-mutated carcinoma cells, adavosertib (Adv), a WEE1 G2 checkpoint kinase (WEE1) inhibitor, has been the recent focus of study (6,7).

WEE1 is a kinase that regulates replication stress and cell cycle arrest at the G2/M checkpoint. DNA damage during the S-phase activates WEE1, which in turn phosphorylates cyclin-dependent kinase 1 (CDK1) at Tyr15 to inactivate its kinase activity (8). Because p53 regulates the G1/S checkpoint (9), *TP53*-mutated cells rely on the G2/M checkpoint to arrest the cell cycle to repair their DNA damage. Therefore, Adv treatment of *TP53*-mutated cells leads to the cells entering M-phase without DNA repair, which in turn causes cell death named mitotic catastrophe. Mitotic catastrophe is a type of cell death characterized by DNA damage, abnormalities in the mitotic apparatus, dysfunction of the mitotic checkpoint, and failure in the occurrence of normal mitosis (10,11), but there is no clear definition. As Adv abrogates cell cycle arrest, it was suggested that the co-administration of DNA-damaging drugs with Adv enhances cytotoxicity (7,12,13). In the present study, we sought to identify drug combinations to enhance Adv-induced cytotoxicity without losing selective cell death in *TP53*-mutated cells.

It has been reported that histone deacetylase (HDAC) inhibitors induce growth arrest, differentiation, and apoptosis *in vitro*, and suppress tumor growth in xenograft mouse models with various cancer cell lines including HNSCC (14-16).

Additionally, HDAC inhibitors have been shown to enhance cytotoxicity in combination with DNA-damaging anticancer drugs (17,18) or Adv (19-21). We recently reported that ricolinostat (RCS), a selective histone deacetylase 6 (HDAC6) inhibitor, exhibits potent cell growth inhibition in HNSCC cell lines *in vitro* in combination with the proteasome inhibitor bortezomib (22). Of note, HDAC6 differs from other HDACs by deacetylating cytoplasmic proteins, including α-tubulin. HDAC6 has also been reported to be involved in the cell cycle via deacetylation of α-tubulin (23). Additionally, inhibition of HDAC6 has been reported to sensitize cancer cells to DNA-damaging drugs (24-26). As the disruption of the cell cycle or DNA damage enhances mitotic catastrophe, in the present study, we assessed the effect of the combined treatment of Adv and RCS on HNSCC cell lines with *TP53* mutation (CAL27, SAS, HSC-3, Detroit562, and OSC-19) or impaired p53 function by HPV-infection (UPCI-SCC154).

## Materials and methods

*Reagents*. Adavosertib (AZD1775, MK-1775, hereafter referred to as Adv) was purchased from MedChemExpress. Ricolinostat (ACY-1215, hereafter referred to as RCS) was purchased from Selleck Chemicals. Adv and RCS were dissolved in dimethyl sulfoxide (DMSO) (Wako Pure Chemical Industries) to make the stock solution at a concentration of 10 mM for Adv and 5 mM for RCS. Doxorubicin (DOX) was purchased from Cayman Chemical Co. z-VAD-fmk was purchased from Peptide Institute (Japan).

*Cell lines and culture conditions*. The human oral squamous cell carcinoma cell line CAL27, the human pharyngeal squamous carcinoma cell line Detroit562, human tongue squamous carcinoma cell line UPCI-SCC154, the human breast mammary gland adenocarcinoma cell lines MCF7 and MDA-MB-231, and the human lung adenocarcinoma cell line A549 were purchased from the American Type Culture Collection (ATCC). The human tongue squamous carcinoma cell lines SAS, HSC-3, and OSC-19 cells were obtained from the JCRB Cell Bank (Osaka, Japan). A549 and MCF7 cells possess wild-type *TP53*. MDA-MB-231, CAL27, HSC-3, SAS, Detroit562, and OSC-19 cells carry mutant *TP53*. UPCI-SCC-154 cells are HPV-positive and show impaired p53 function. CAL27, Detroit562, MCF7, MDA-MB-231, and A549 cells were cultured in Dulbecco's modified Eagle medium (DMEM) supplemented with 10% fetal bovine serum (FBS; Biosera) and 1% penicillin/streptomycin solution (Wako Pure Chemical Industries). UPCI-SCC154 cells were cultured in MEM supplemented with 10% FBS and 1% penicillin/streptomycin solution. SAS and OSC-19 cells were cultured in DMEM/ F12 medium supplemented with 10% FBS and 1% penicillin/streptomycin solution. HSC-3 cells were cultured in Eagle's minimum essential medium (EMEM) supplemented with 10% FBS and 1% penicillin/streptomycin solution. All cell lines were cultured at 37˚C in a humidified incubator containing 5% $CO_2$ and 95% air. In all experiments, as a control, cells were treated with control medium containing less than 1% DMSO to match the amount of solvent brought in by the drug. All cell line experiments were conducted within 10 passages after thawing. Mycoplasma contamination was tested routinely using the e-Myco™ Mycoplasma PCR Detection kit ver.2.0 (iNtRON Biotechnology, Inc.).

*Establishment of TP53-KO A549 and TP53-KO MCF7 cells*. TP53-KO A549 cells were established as previously described (27). Briefly, A549 cells were transfected with pSpCas9 (BB)-2A-Puro (PX459) V2.0 plasmid vector (a gift from Dr Feng Zhang; plasmid cat. no. 48139; Addgene) with the following sequence (5'-CACCGTCCATTGCTTGGGACG GCAA-3'), selected with puromycin for 2 days, and grown without puromycin to select single colonies. TP53-KO MCF7 cells were also established in the same way.

*Establishment of CAL27/H2B-mCherry/AcGFP-α-tubulin cells*. To establish CAL27 cells expressing H2B-mCherry and AcGFP-α-tubulin, CAL27 cells were infected with lentiviruses and positive clones were selected using puromycin and blasticidin. Lentiviruses were produced in 293T cells (ATCC) by transfection of the following plasmids: pMD2.G (gift from Dr Didier Trono: Addgene #12259), psPAX2 (gift from Dr Didier Trono: Addgene #12260), pLenti6-H2B-mCherry (gift from Dr Torsten Wittmann: Addgene plasmid #89766) (28), and pLenti-AcGFP-α-tubulin. For pLenti-AcGFP-α-tubulin construction, TUBA1A cDNA was cloned into pAcGFP1-Hyg-C1 vector (Takara Bio Inc.), and then, the AcGFP-α-tubulin fused gene was inserted into the pLentiN vector (gift from Dr Karl Munger: Addgene #37444) (29).

*RNA interference*. For the gene silencing of HDAC6 in CAL 27 cells, HDAC6 siRNA and control siRNA were synthesized as follows (Japan Bio Services Co., Ltd.): siHDAC6#2: sense GCUUAUUUAAGUGUUAAUAdTdT and antisense UAU UAACACUUAAAUAAGCdAdC; siHDAC6#3: sense GGU UUUUGCUUUUUCAACUdTdT and antisense AGUUGA AAAAGCAAAAACCdGdC; siHDAC6#4: sense GCAUAU GUAAUAAAGUACAdTdT and antisense UGUACUUUA UUACAUAUGCdAdA; control siLuc: sense CUUACG CUGAGUACUUCGAdTdT and antisense UCGAAGUAC UCAGCGUAAGdTdT. siRNAs were diluted to 200 nM in Opti-MEM I (Thermo Fisher Scientific, Inc.). Transfection was performed using Lipofectamine RNAiMAX transfection reagent (Thermo Fisher Scientific, Inc.) according to the manufacturer's instructions. Knockdown (KD) efficiency was assessed using western blotting.

*Assessment of cell death*. The dead cell counts were assessed by staining with propidium iodide (PI) (FUJIFILM Wako Chemical Corp.), and the number of red fluorescent signals was counted using the IncuCyte ZOOM (Sartorius) automated live cell imaging system. The cells were treated with Adv with or without RCS in the presence of PI (2.5 $\mu$g/ml) for up to 48 h in 96-well plates in tetraplicate (30).

*Morphological assessment*. The cells were spread on glass slides using a Cytospin 4 Centrifuge (Thermo Fisher Scientific, Inc.) to prepare glass slides, stained with May-Grünwald-Giemsa and examined under a digital microscope (BZ-X800; KEYENCE Co.).

*Western blotting*. The cells were lysed using RIPA lysis buffer (Nacalai Tesque) added together with a protease and phosphatase inhibitor cocktail (Nacalai Tesque). Equal amounts of proteins (25 $\mu$g) were loaded onto the gels (7.5, 10 and 15% gels were used), separated by SDS-PAGE, and then transferred onto Immobilon-P membranes (Millipore Corp.). These membranes were probed with primary antibodies, such as anti-p53 antibody (Ab) (sc-126, 1/1,000), anti-β-actin Ab (sc-47778, 1/1,000), anti-HDAC6 Ab (sc-11420, 1/1,000), anti-acetylated α-tubulin Ab (sc-23950, 1/1,000), and anti-α-tubulin Ab (sc-5286, 1/1,000) were purchased from Santa Cruz Biotechnology, Inc. Anti-PARP Ab (#9542S, 1/1,000), anti-caspase3 Ab (#9665S, 1/1,000), anti-phospho-p53 Ab (#9286, 1/1,000), anti-p21 Ab (#2947S, 1/1,000), anti-phospho-ATR Ab (#9947, 1/1,000), anti-ATR Ab (#2790, 1/1,000), anti-phospho-Chk1 (Ser345) Ab (#2348, 1/1,000), anti-Chk1 Ab (#2360, 1/1,000), anti-phospho-Chk2 (Thr68) Ab (#2197, 1/1,000), anti-Chk2 Ab (#3440, 1/1,000), anti-phospho-Cdc2 (Tyr15) Ab (#4539, 1/1,000), anti-Cdc2 Ab (#9116, 1/1,000), anti-H2A.X Ab (#7631, 1/1,000), and anti-phospho-histone H2A.X (Ser139) Ab (#9718, 1/1,000) were purchased from Cell Signaling Technology, Inc.

*Assessment of mitotic catastrophes*. CAL27/H2B-mCherry/AcGFP-α-tubulin cells were seeded on collagen-coated glass-bottom dishes (CELLview #627870, Greiner). The next day, the cells were treated with control medium, Adv, RCS, or Adv + RCS, and time-lapse images were obtained every 10 min using a confocal microscope LSM 700 equipped with $CO_2$, temperature, and humidity controller (Carl Zeiss) or fluorescent microscope BZ-X800 equipped with a time-lapse module (BZ-H4XT) (KEYENCE). The cells were maintained at 37˚C and 5% $CO_2$, under humidified conditions. Time-lapse images from fluorescent microscopy were used to analyze the cell fate.

*Statistical analysis*. All quantitative data are expressed as mean ± standard deviation (SD). Statistical analyses for cell death inhibition with z-VAD-fmk treatment, and cell death in combination with Adv treatment and HDAC6 KD were performed using two-way ANOVA followed by Bonferroni's multiple comparison test. For the analysis of the M-phase duration, the Kruskal-Wallis test followed by Dunn's multiple comparison test was used. Statistical significance was set at $P<0.05$. All analyses were performed using GraphPad Prism 5 software (GraphPad Software, Inc.). The synergistic effect was assessed as follows. Based on nesting all elapsed hours for each experiment, mixed-effect linear regression analyses were performed by setting the number of cell deaths as the dependent variables and the concentration of the two anticancer drugs as independent variables. To assess the possible synergistic effects of the two drugs, the interaction term was added as one of the independent variables in the model to calculate p-for-interaction. All statistical analyses were performed using Stata version 17.0 (Stata Corp.). When the mono treatment was enough to kill almost all cells, the analysis indicated an 'antagonistic effect', because the dead cell count in the combination treatment group was smaller than the dead cell count in each mono treatment group.

## Results

*Combined treatment of Adv and RCS synergistically induces cell death in TP53-mutated HNSCC cells*. To assess the effect of the combined treatment of Adv and RCS on *TP53*-mutated HNSCC cells, namely CAL27, HSC-3, SAS, Detroit562, and OSC-19 cells, and HPV-positive UPCI-SCC-154 cells, which showed impaired p53, these cells were treated with Adv and RCS for 48 h and PI-positive dead cell number was measured using a live cell imaging system. In HNSCC cells, treatment with Adv and/or RCS induced cell death in a dose- and time-dependent manner. Notably, co-administration of Adv and RCS synergistically enhanced cell death in four out of five *TP53*-mutated HNSCC cell lines (except Detroit562 cells) as well as in the HPV-positive UPCI-SCC-154 cell line (Figs. 1 and S1). To address whether this synergistic effect was ubiquitous, breast cancer cell lines (MDA-MB-231 and MCF7) and a lung cancer cell line (A549) were also treated with Adv and/or RCS for 48 h (Figs. 1 and S1). Although co-administration of RCS with Adv led to enhanced cell death in MDA-MB-231 cells with *TP53* mutation, little or no enhanced cell death was observed in MCF7 and A549 cells, both carrying wild-type *TP53*. Because Adv has been reported to induce mitotic catastrophe in *TP53*-mutated cells, we hypothesized that RCS enhanced Adv-induced mitotic catastrophe in *TP53*-mutated cells but not in wild-type *TP53* cells. To address this issue, we next compared the induction of cell death between *TP53* wild-type and *TP53* knockout (KO) A549 cells, which were established using the CRISPR-Cas9 system (Fig. 2A). Although TP53-KO A549 cells did not show altered sensitivity to Adv as compared to wild-type A549 cells, co-administration of RCS significantly enhanced cell death in TP53-KO but not TP53-WT A549 cells (Fig. 2B). To further confirm this observation, we established TP53-KO MCF7 cells using the CRISPR-Cas9 system (Fig. S2A). Although wild-type MCF7 cells showed slight synergistic cell death in the combined treatment of Adv and RCS, TP53-KO MCF7 cells showed increased synergistic cell death by the combined treatment as shown in A549 cells (Fig. S2B). This indicated that the combination treatment of Adv and RCS can synergistically induce cell death in cells lacking p53 function.

*Combined treatment of Adv and RCS in cancer cells leads to mitotic catastrophe*. To identify the mechanism by which the combined treatment of Adv and RCS leads to enhanced cell death, we treated CAL27 cells with Adv and RCS for 24 h and observed their cell morphology. In response to drug treatment, CAL27 cells showed nuclear fragmentation and chromatin condensation (Fig. 3A), which are characteristic features of cells undergoing apoptosis. Western blotting revealed that Adv or RCS treatment induced the cleavage of caspase-3, and co-administration of the two drugs further increased the cleavage of caspase-3 in CAL 27 cells (Fig. 3B). Additionally, Adv-and RCS-induced cell death was abolished in the presence of a pan-caspase inhibitor, z-VAD-fmk (Fig. 3C). These data demonstrated that co-administration of Adv and RCS induced apoptosis. Adv is known to induce mitotic catastrophe, which subsequently leads to apoptotic or non-apoptotic cell death (31). To investigate whether the co-administration of Adv and RCS enhanced mitotic catastrophe, we established

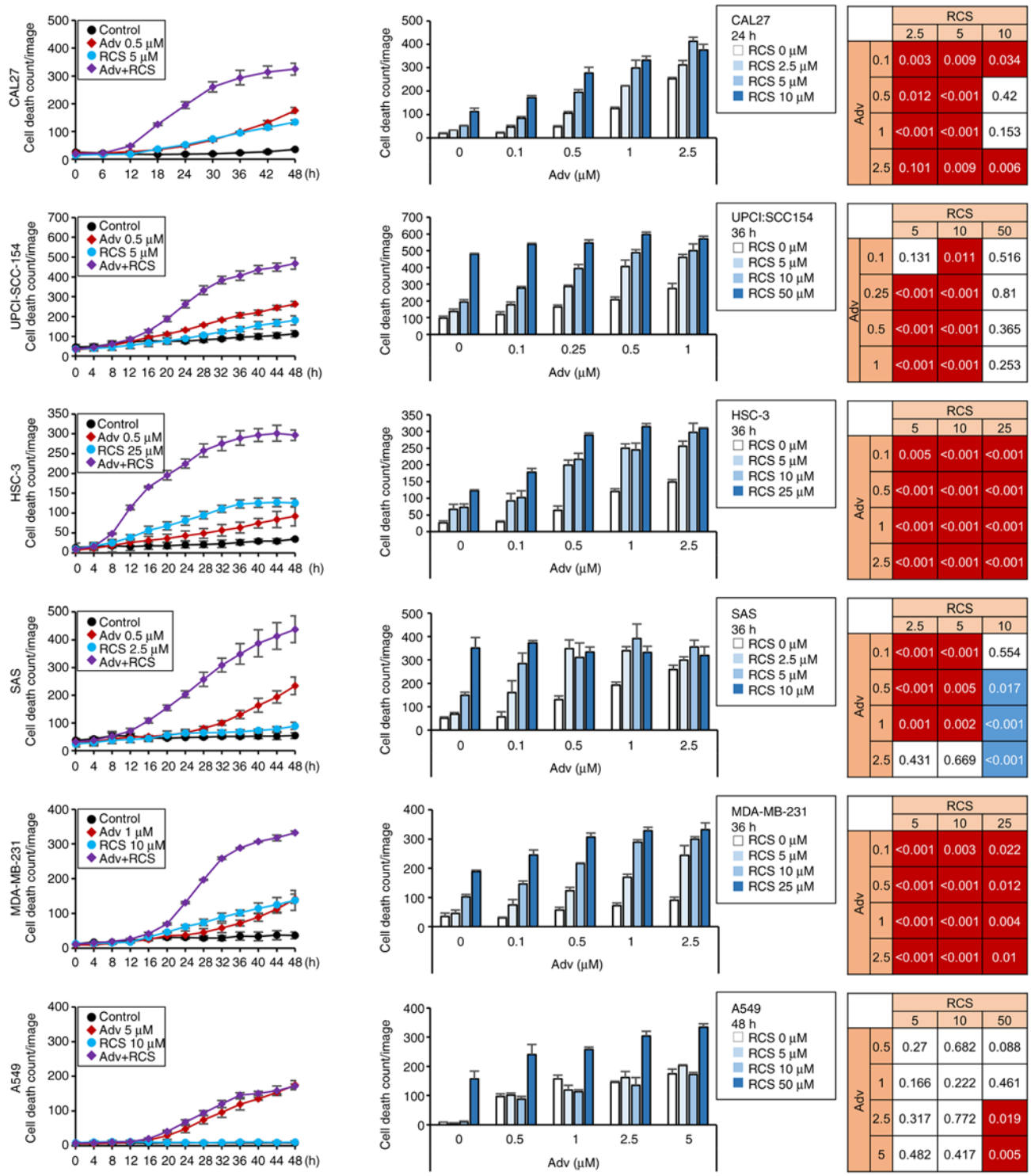


Figure 1. Ricolinostat enhances adavosertib-induced cytotoxicity in HNSCC cell lines. CAL27, UPCI-SCC-154, HSC-3, SAS, MDA-MB-231, and A549 cells were treated with Adv in combination with RCS for up to 48 h. Cells were monitored using IncuCyte live cell imaging system, and dead cell number was assessed using PI staining. Time-dependent and dose-dependent cell death numbers are shown in the left and the middle panels, respectively. Representative data of three independent experiments are shown. n=3, bar, mean ± SD. Synergistically enhanced cell death in the combination treatment was analyzed as described in Materials and methods and summarized in the right panels. A significant synergistic effect with both Adv and RCS treatment with P<0.05 is shown in red. An antagonistic effect with P<0.05 is shown in blue. HNSCC, head and neck squamous cell carcinoma; Adv, adavosertib; RCS, ricolinostat.

CAL27 cells stably expressing AcGFP-α-tubulin and histone-H2B-mCherry to monitor mitosis. Time-lapse imaging showed that most cells treated with Adv could not complete mitosis and underwent cell death, which indicated mitotic catastrophe (Fig. 3D-F). Additionally, Adv treatment resulted in a prolonged duration of mitosis (Fig. 3G). On the contrary, although RCS treatment induced cell death, most of the cell death occurred during interphase, and most RCS-treated cells did not enter metaphase (Fig. 3E and F). This indicated that, unlike Adv, RCS hardly induced mitotic

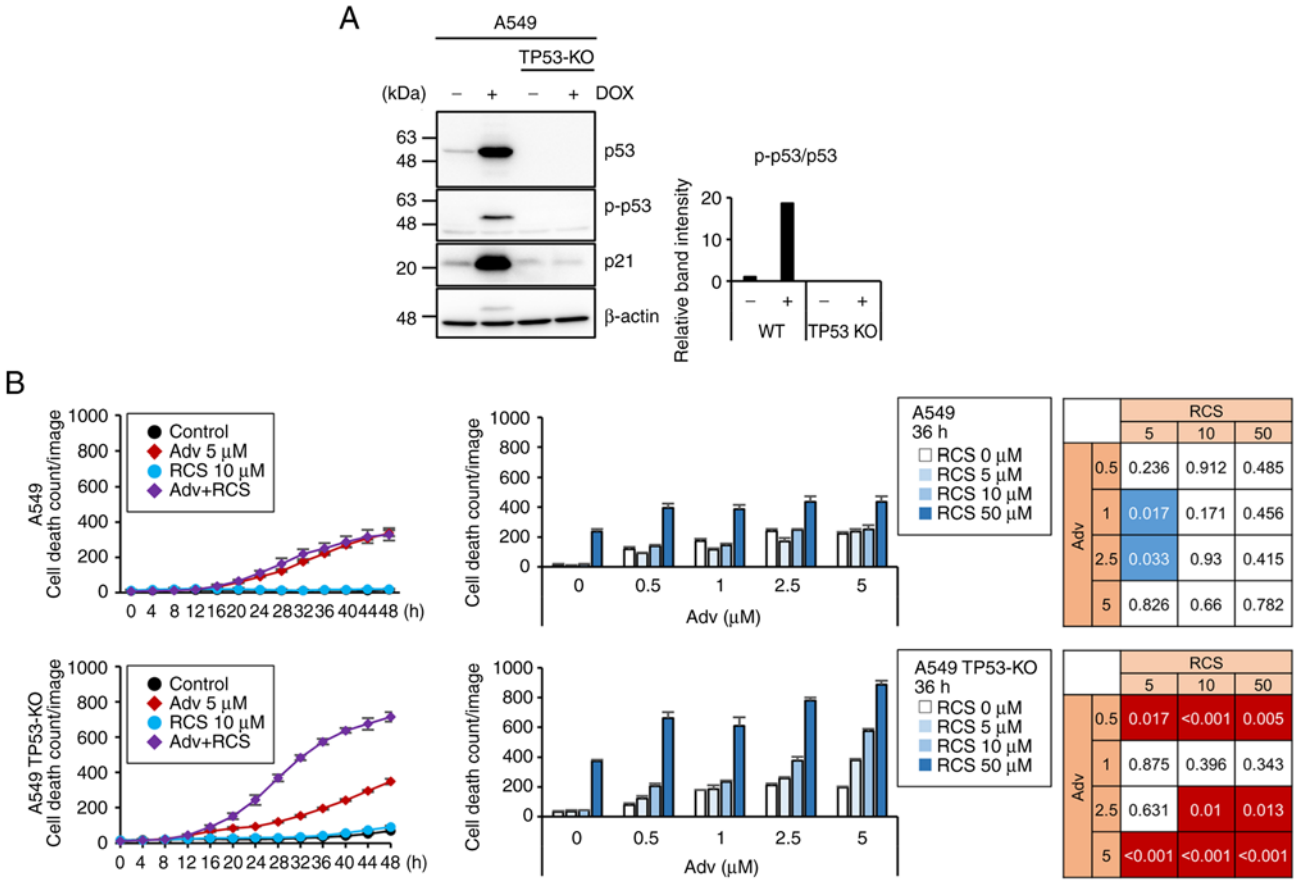


Figure 2. Combined treatment of adavosertib and ricolinostat enhances cell death only in TP53-KO A549 cells. (A) TP53 KO in A549 cells was confirmed by western blotting. Expression of p53, phospho-p53, and p21 was assessed after doxorubicin (DOX) (1 $\mu$M) treatment for 24 h. β-actin was used as a loading control. Relative band intensity of p-p53/p53 was calculated and is summarized in the right panel. (B) TP53-WT and TP53-KO A549 cells were treated with Adv in combination with RCS for up to 48 h. Cells were monitored using IncuCyte live cell imaging system, and dead cell number was assessed by PI staining. Dose-dependent and time-dependent cell death numbers are shown. The synergistic effect on cell death in combination treatment was assessed and is summarized at the right. Representative data of three independent experiments are shown. n=3, bar, mean ± SD. Adv, adavosertib; RCS, ricolinostat.

catastrophe. Of note, when CAL27 cells were simultaneously exposed to Adv and RCS, dead cell counts were increased and most of the cell death occurred during mitosis (Fig. 3D-F). However, the duration of the mitotic phase until cell death was not further extended as compared to the cells treated with Adv alone (Fig. 3G). These data showed that RCS enhanced the Adv-induced mitotic catastrophe.

*RCS promotes Adv-induced mitotic entry along with the increment of γ-H2A.X expression*. Next, to address how RCS enhances Adv-induced mitotic catastrophe, we assessed the G2/M checkpoint and DNA damage response (DDR)-related proteins by western blotting in CAL27 cells (Fig. 4A). WEE1, a Ser/Thr protein kinase family member, phosphorylates CDK1 at Tyr15, inhibits its activity, and acts as a negative regulator for entry into mitosis (G2 to M transition) (32). Thus, Adv treatment decreased CDK1 (Tyr15) phosphorylation (Fig. 4A). This indicated that CDK1 was activated, leading to premature mitotic entry. At the same time, we observed increased phosphorylation of Chk1 (Ser345), which indirectly inactivates CDK1. This increased p-Chk1 presumably compensated for the increased CDK1 activity. In contrast, RCS treatment suppressed Chk1 phosphorylation. Thus, co-administration of RCS with Adv suppressed p-Chk1 and p-CDK1. This appeared to further promote forced mitotic entry to induce mitotic catastrophe. In support of these findings, co-administration of the two drugs resulted in further increase in γ-H2A.X expression, a marker of DNA double-strand breaks. These data suggest that RCS enhanced Adv-induced mitotic catastrophe by suppressing p-Chk1 and p-CDK1 (Fig. 4A).

As shown in Fig. 1, the pronounced cell death induction by combined treatment of Adv and RCS appeared to be dependent on *TP53* mutations. We examined whether the co-administration of RCS suppressed p-Chk1 in both WT and TP53-KO A549 cells (Fig. 4B). In both cells, Adv treatment increased p-Chk1 and suppressed p-CDK1, similar to that observed in CAL27 cells. Although co-administration of RCS with Adv suppressed p-CDK1 and p-Chk1 in both cell lines, γ-H2A.X expression was increased only in TP53-KO A549 cells. This may reflect the dependency of *TP53*-mutated cells on the G2/M checkpoint. These data also suggest that RCS enhances premature mitotic entry by suppressing p-Chk1 in A549 cells. Additionally, we assessed the DDR-related protein expression in Detroit562 cells which carry mutated-*TP53* but did not show pronounced cell death by combined treatment of Adv and RCS. Detroit562 cells showed almost the same result as WT A549 cells and failed to further upregulate γ-H2A.X expression as compared to treatment with Adv alone (Fig. S3).

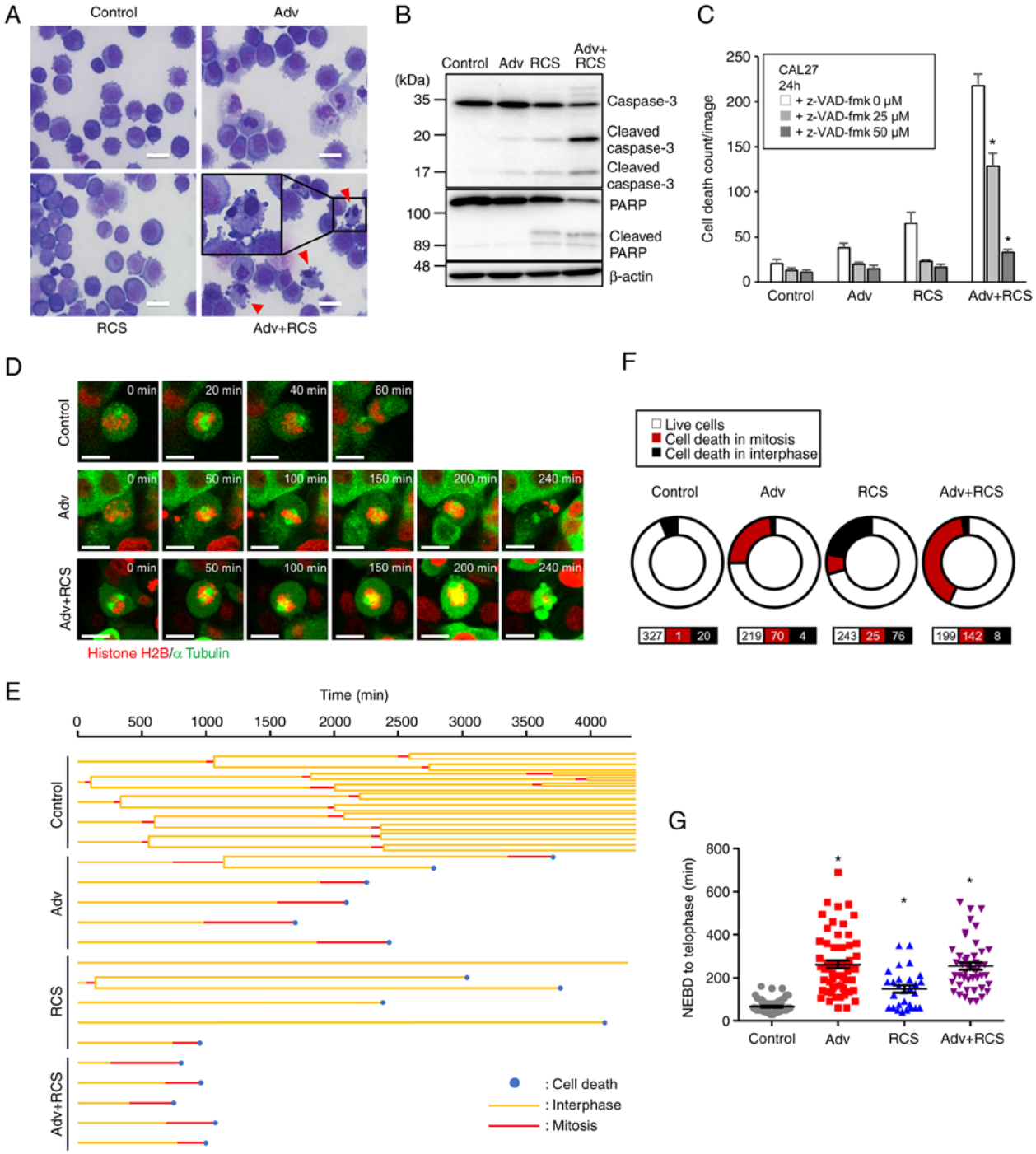


Figure 3. Co-administration of ricolinostat enhances adavosertib-induced mitotic catastrophe in CAL27 cells. (A) CAL27 cells were treated with control, Adv (0.5 $\mu$M), RCS (5 $\mu$M), or Adv+RCS for 24 h and then stained with May-Grünwald-Giemsa stain. Scale bar, 25 $\mu$m. Arrowheads indicate nuclear chromatin condensation. (B) CAL27 cells were treated with control, Adv (0.5 $\mu$M), RCS (5 $\mu$M), and Adv + RCS for 24 h, and then, cleavage of PARP and caspase-3 were assessed by western blotting. (C) CAL27 cells were treated with control, Adv (0.5 $\mu$M), RCS (5 $\mu$M), or Adv + RCS in the presence of z-VAD-fmk (0, 25, and 50 $\mu$M) for 24 h, and dead cell number was monitored using IncuCyte live cell imaging system by PI staining. n=7, bar, mean ± SD; $^{*}$P<0.05 vs. 0 $\mu$M z-VAD-fmk. (D) Live cell imaging of CAL27 cells expressing AcGFP-α-tubulin and Histone H2B-mCherry. Cells were treated with control, Adv (0.5 $\mu$M), or Adv + RCS (5 $\mu$M) and monitored using confocal microscopy. Representative images of cells after the nuclear envelope breakdown (NEBD) are shown. Time after the NEBD is shown in the upper right corner of each image. Scale bar, 20 $\mu$m. (E) Five representative cell fates in each treated cell with control, Adv (0.5 $\mu$M), RCS (5 $\mu$M), or Adv + RCS are shown in a tree diagram. (F) The ratio of cell death in mitosis or interphase in each treated cell is summarized in the pie chart. n for each condition is shown at the bottom. Data from three independent experiments are summarized. (G) Time from NEBD to telophase or cell death was assessed and summarized. n=75, 59, 29, 46. Data from three independent experiments are summarized. $^{*}$P<0.05 vs. the control. PARP, poly(ADP-ribose) polymerase; Adv, adavosertib; RCS, ricolinostat.

This suggests that some of the *TP53*-mutated cell lines may have gained a compensatory mechanism to p53 and are insensitive to co-administration of RCS with Adv.

*RCS enhanced cell death induction via inhibition of HDAC6.* It has been reported that although RCS selectively inhibits HDAC6 ($IC_{50}$=4.7 nM), it also inhibits HDAC1, 2, and 3

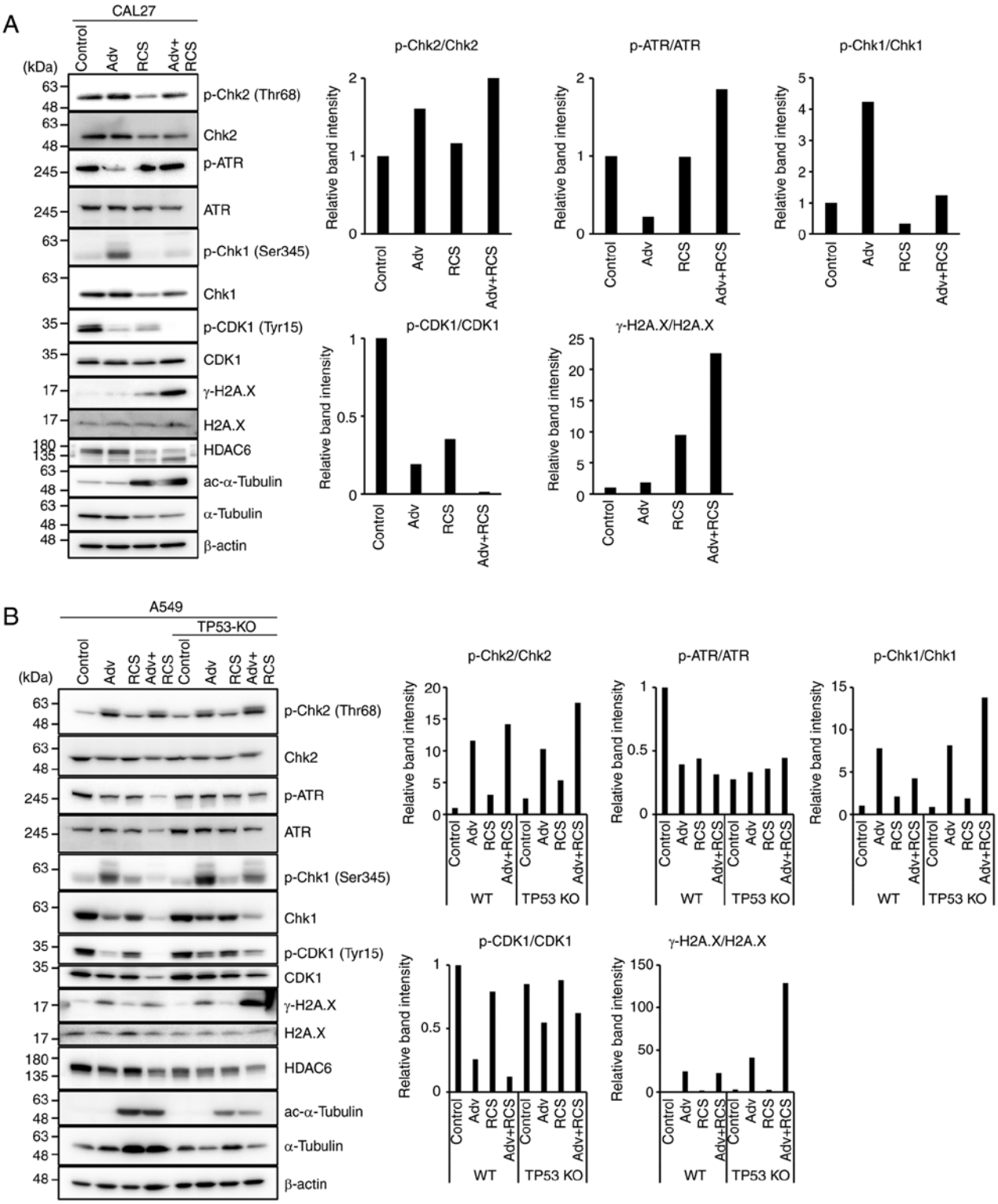


Figure 4. Ricolinostat suppresses phosphorylation of Chk1 and further suppresses p-CDK1 when co-administered with adavosertib. (A) CAL27 cells and (B) TP53-WT and TP53-KO A549 cells were treated with Adv (0.5 $\mu$M), RCS (5 $\mu$M), and Adv+RCS for 24 h (CAL27 cells) or 48 h (A549 cells), and then the expression of DNA damage response-related proteins (p-Chk2, Chk2, p-ATR, ATR, p-Chk1, Chk1, p-CDK1, CDK1, and γ-H2A.X) was assessed by western blotting. To assess the inhibitory effect of HDAC6 by RCS, the level of acetylated (ac)-α-tubulin was monitored. Expression of β-actin was assessed as the loading control. The relative band intensity of each phosphorylated protein was calculated and summarized at the right. Representative data of three independent experiments are shown. Adv, adavosertib; RCS, ricolinostat; WT, wild-type; Chk, checkpoint kinase; ATR, ATR serine/threonine kinase; CDK1, cyclin-dependent kinase 1.

($IC_{50}$=58, 48, and 51 nM, respectively) at higher concentrations (33). To clarify whether the enhanced cell death mediated by RCS was due to the inhibition of HDAC6, we knocked down HDAC6 using three different siRNAs (siHDAC6 #2, #3, and #4). All three siRNAs efficiently knocked down HDAC6 and increased acetylated α-tubulin, which is a substrate for

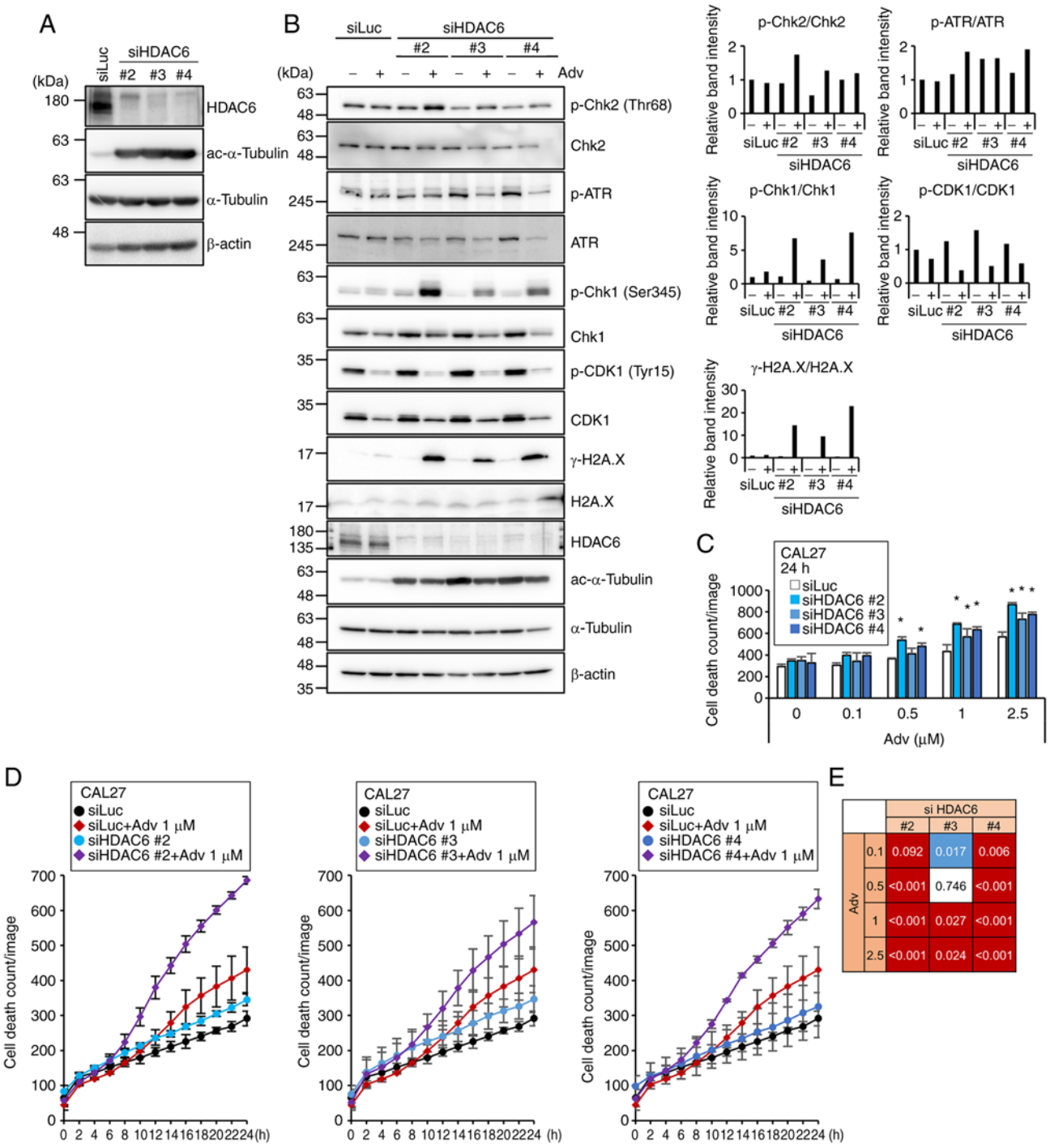


Figure 5. HDAC6 knockdown (KD) enhances adavosertib-induced cell death in CAL27 cells. (A) Knockdown efficiency of HDAC6 in CAL27 cells with three different HDAC6 siRNAs was assessed by western blotting. (B) CAL27 cells were transfected with siLuc or three different siHDAC6 siRNAs (#2-4) and then treated with or without Adv (1 μM) for 24 h. Expression of DDR-related proteins was detected by western blotting. Expression of HDAC6 and acetylated (ac)-α-tubulin were monitored to assess the KD efficiency. Representative data of three independent experiments are shown. (C and D) CAL27 cells were transfected with siLuc or three different siHDAC6 siRNAs (#2-4) and then treated with various concentrations of Adv up to 24 h. Cells were monitored using IncuCyte live cell imaging system, and dead cell number was assessed using PI staining. Dose-dependent (C) and time-dependent (D) cell death numbers are shown. Representative data of three independent experiments are shown. n=3, bar, mean ± SD. *P<0.05 vs. siLuc. (E) The synergistic effect of cell death in the combination of Adv treatment and HDAC6 KD shown in (C) and (D) was assessed and is summarized. Adv, adavosertib; RCS, ricolinostat; HDAC6, histone deacetylase 6; DDR, DNA damage response.

HDAC6 (Fig. 5A). Although KD of HDAC6 by itself did not change p-Chk1 levels or γ-H2A.X expression levels, Adv treatment in HDAC6-KD cells resulted in increased γ-H2A.X expression, as in the case of CAL27 cells treated with RCS and Adv (Fig. 5B). However, we did not observe the suppression of p-Chk1 or p-CDK1 in Adv-treated HDAC6-KD cells. In terms of cell death induction, treatment with Adv in HDAC6-KD cells significantly and synergistically increased cell death, as in the case of CAL27 cells concomitantly treated with RCS and Adv (Fig. 5C-E). This suggested that increased DNA

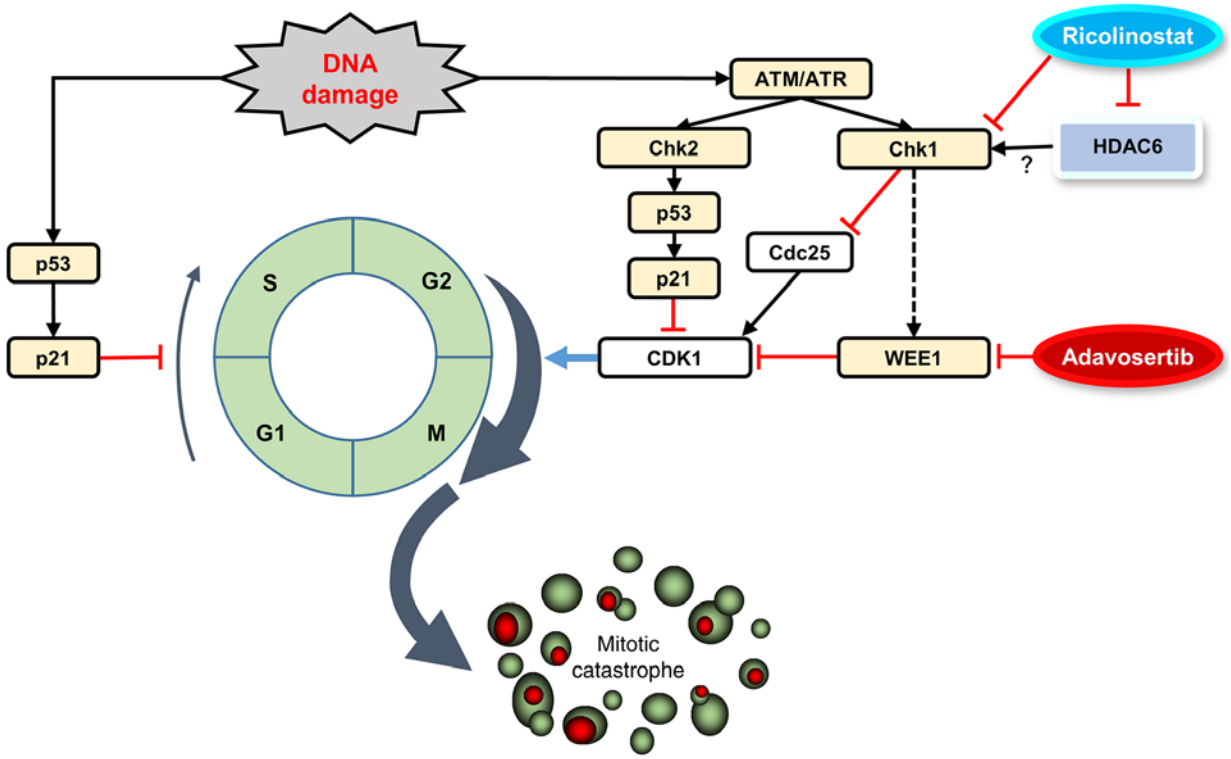


Figure 6. Schema of the effect of adavosertib and ricolinostat on the G2/M checkpoint. In *TP53*-mutated cells, DNA repair is dependent on the G2/M checkpoint regulated by CDK1. CDK1 is a key regulator inducing cell cycle progression through the G2/M checkpoint. WEE1 phosphorylates and inhibits CDK1. Adavosertib inhibits WEE1 and then CDK1 is dephosphorylated and activated. Chk1 inhibits Cdc25, which dephosphorylates and activates CDK1. Ricolinostat decreases the phosphorylation of Chk1, indicating inhibition of Chk1. Chk, checkpoint kinase; ATR, ATR serine/threonine kinase; ATM, ATM serine/threonine kinase; CDK1, cyclin-dependent kinase 1; HDAC6, histone deacetylase 6; WEE1, WEE1 G2 checkpoint kinase.

damage and enhanced cell death by co-administration of RCS with Adv appeared to have been caused by HDAC6 inhibition, but the enhanced mitotic catastrophe caused by RCS addition to Adv treatment may be independent of HDAC6 inhibition.

## Discussion

In the present study, the combined WEE1 G2 checkpoint kinase (WEE1) inhibitor adavosertib (Adv) and the histone deacetylase 6 (HDAC6)-selective inhibitor ricolinostat (RCS) treatment exhibited synergistic cytotoxicity in *TP53*-mutated, impaired p53 function by HPV-infection, or TP53-KO HNSCC, lung cancer, and breast cancer cell lines likely via enhanced induction of Adv-induced mitotic catastrophe (Fig. 6). WEE1 phosphorylates the amino acids Tyr15 and Thr14 of CDK1, which keeps the kinase activity of CDK1 low and prevents entry into mitosis (32). As p53 regulates the G1/S checkpoint, *TP53*-mutated cells rely on the G2/M checkpoint to arrest the cell cycle to repair their DNA damage. Thus, *TP53*-mutated cells with increased replication stress appeared to exhibit greater sensitivity to WEE1 inhibitors (34,35). The synergistic effect of the two-drug combination shown in Fig. 1 appeared to be mediated through forced entry of the cell into M phase by CDK1 activation. Indeed, the two-drug combination resulted in enhanced dephosphorylation of CDK1, which is an active state of CDK1, as compared to that in the treatment of Adv alone. This was accompanied by pronounced γ-H2A.X expression, which indicated an increase in DNA double-strand breaks in *TP53*-mutated cells (Fig. 4A and B). In Adv-treated cells, a compensatory mechanism appeared to be induced, leading to an increased expression of p-Chk1. However, combination treatment with RCS suppressed p-Chk1 upregulation and further activated CDK1 to promote premature mitotic entry (Figs. 4 and 6).

Adv is an orally available, first-in-class, reversible WEE1 inhibitor (36). Most clinical trials using WEE1 inhibitors have been conducted as a combination with chemotherapy or radiotherapy (37-40). In the case of WEE1 inhibitor monotherapy against recurrent uterine serous carcinoma, which frequently possesses *TP53* mutation, the treatment showed significant elongation of progression-free survival (PFS) and a high response rate (41). Consistent with our results (Figs. 1 and 2), several previous studies have reported that sensitivity to Adv is dependent on *TP53* mutation status (6,7,42), whereas a few other reports have shown that *TP53* status does not alter sensitivity to Adv (43). This may suggest that *TP53* single gene mutation by itself is not sufficient to determine sensitivity to WEE1 inhibitor monotherapy.

HDAC6 is a unique member of the HDAC subfamily possessing two catalytic domains, namely DAC1 with E3-ligase activity and DAC2 with deacetylase activity (44). HDAC6 deacetylates histones; however, cytoplasmic proteins, namely α-tubulin, cortactin, and heat shock protein 90 (HSP90), are also deacetylated by HDAC6 (45-47). The roles of HDAC6 in tumorigenesis and cell-cycle progression have been reported (23,48,49). The overexpression of HDAC6 has been reported in acute myeloid leukemia, oral squamous cell carcinoma, and ovarian cancer (50-52), and higher HDAC6

expression appears to correlate with tumor progression and malignancy in hepatocellular carcinoma and esophageal squamous cell carcinoma (53,54). In our study, HDAC6 inhibition by RCS suppressed cell cycle progression (Fig. 3), which was consistent with previous reports showing that RCS or other HDAC inhibitors caused G2/M phase arrest (53,55). In contrast, in the presence of Adv + RCS, the cells underwent a pronounced mitotic catastrophe, indicating increased entry into the M-phase. The molecular mechanisms underlying this contradictory phenomenon remain unclear.

Our study demonstrated that HDAC6 inhibition by RCS suppressed p-Chk1 expression (Fig. 4A and B), whereas HDAC6 KD slightly increased Chk1 (Fig. 5B). Thus, suppression of p-Chk1 by RCS seemed to be HDAC6-independent. However, as described above, in addition to deacetylase activity, HDAC6 possesses E3-ligase activity, which ubiquitinates and degrades Chk1 and functions in DDR. Therefore, it was reported that HDAC6 deletion resulted in an increase in Chk1, which enhanced radiation-induced cell cycle arrest in non-small cell lung cancer cells (44). In our system, although HDAC6 KD suppressed both activities, RCS interacted only with DAC2 and E3-ligase activity localized in DAC1 appeared to be intact. If the increase in Chk1 due to DAC1 inhibition overcomes the inhibition of p-Chk1 caused by DAC2 inhibition, the HDAC6 KD experiment alone is not sufficient to determine whether RCS suppresses p-Chk1 via HDAC6. To address this, we need to further evaluate the specific disruption/deletion of the DAC2 domain in HDAC6.

In terms of the Chk1-CDK1 axis, Adv treatment of HDAC6-KD cells resulted in increased γ-H2A.X and cell death despite no decrease in p-Chk1 or p-CDK1 (Fig. 5). This indicates that the enhanced cell death by siHDAC6 or RCS is not limited to be mediated by Chk1-CDK1. As previously reported, we also showed that RCS treatment and HDAC6 KD resulted in α-tubulin acetylation (Figs. 4 and 5) (45). It is well-known that post-translational modifications of tubulins contribute to microtubule dynamics, which are crucial for proper spindle organization and cell cycle progression (56). CYLD, a tumor suppressor gene product, has been reported to bind and inactivate HDAC6 along with increased acetylation of tubulin, which negatively regulates cell-cycle progression (23). In addition, tubastatin A, an HDAC6 inhibitor, has been reported to disrupt maturational progression and meiotic apparatus assembly in mouse oocytes (57). Therefore, it is still possible that HDAC6 inhibitors including RCS cause abnormal mitosis by constitutively enhancing the acetylation of tubulins, leading to disruption of microtubule dynamics. This may also play a role in promoting the Adv-induced mitotic catastrophe.

To the best of our knowledge, this is the first report showing that RCS with a higher selectivity against HDAC6 suppresses p-Chk1. Although suppression of p-Chk1 by RCS may be independent of HDAC6, enhanced DNA damage and cell death were observed in both RCS-treated and HDAC6-KD cells in combination with Adv treatment. As prominent cell death in Adv + RCS-treated cells was only observed in *TP53*-mutated and TP53-KO cells, this drug combination appears to be much less toxic to normal cells with intact *TP53* than in *TP53*-mutated cancer cells. Applying this drug combination in the experiment with the tumor xenograft model appears to have potential for future research. Although *in vivo* studies remain to be carried out, this drug combination with high specificity for cells lacking p53 function could be a good candidate for the treatment of HNSCC patients carrying *TP53* mutations as well as human papillomavirus (HPV)-positive HNSCC patients lacking p53 function.

**Acknowledgements**

Not applicable.

**Funding**

This study was supported by JSPS KAKENHI Grant Number 20K07298 (to NT) and the Cancer Research Grant afforded by the Tokyo Medical University Cancer Research Foundation (to KM).

**Availability of data and materials**

The datasets used during the present study are available from the corresponding authors upon reasonable request.

**Authors' contributions**

KM (Miyazawa) and NT conceived and designed the present study. KM (Miyake), NT and HK (Kazama) performed the experiments. KM (Miyake), NT and HK (Kikuchi) analyzed, interpretated the data. KM (Miyake), NT and KM (Miyazawa) confirmed the integrity of the data. KM (Miyazawa), NT, MH, KT and KM (Miyake) wrote, reviewed and/or revised the manuscript. All authors read and approved the manuscript and agree to be accountable for all aspects of the research in ensuring that the accuracy or integrity of any part of the work are appropriately investigated and resolved.

**Ethics approval and consent to participate**

Not applicable.

**Patient consent for publication**

Not applicable.

**Competing interests**

The authors declare that they have no competing interests.

**References**

1. Bray F, Ferlay J, Soerjomataram I, Siegel RL, Torre LA and Jemal A: Global cancer statistics 2018: GLOBOCAN estimates of incidence and mortality worldwide for 36 cancers in 185 countries. CA Cancer J Clin 68: 394-424, 2018.
2. Agrawal N, Frederick MJ, Pickering CR, Bettegowda C, Chang K, Li RJ, Fakhry C, Xie TX, Zhang J, Wang J, *et al*: Exome sequencing of head and neck squamous cell carcinoma reveals inactivating mutations in NOTCH1. Science 333: 1154-1157, 2011.
3. Stransky N, Egloff AM, Tward AD, Kostic AD, Cibulskis K, Sivachenko A, Kryukov GV, Lawrence MS, Sougnez C, McKenna A, *et al*: The mutational landscape of head and neck squamous cell carcinoma. Science 333: 1157-1160, 2011.
4. Wang X and Sun Q: TP53 mutations, expression and interaction networks in human cancers. Oncotarget 8: 624-643, 2017.

5. Scheffner M, Werness BA, Huibregtse JM, Levine AJ and Howley PM: The E6 oncoprotein encoded by human papillomavirus types 16 and 18 promotes the degradation of p53. Cell 63: 1129-1136, 1990.
6. Indovina P and Giordano A: Targeting the checkpoint kinase WEE1: Selective sensitization of cancer cells to DNA-damaging drugs. Cancer Biol Ther 9: 523-525, 2010.
7. Hirai H, Arai T, Okada M, Nishibata T, Kobayashi M, Sakai N, Imagaki K, Ohtani J, Sakai T, Yoshizumi T, *et al*: MK-1775, a small molecule Wee1 inhibitor, enhances anti-tumor efficacy of various DNA-damaging agents, including 5-fluorouracil. Cancer Biol Ther 9: 514-522, 2010.
8. Den Haese GJ, Walworth N, Carr AM and Gould KL: The Wee1 protein kinase regulates T14 phosphorylation of fission yeast Cdc2. Mol Biol Cell 6: 371-385, 1995.
9. Sancar A, Lindsey-Boltz LA, Unsal-Kaçmaz K and Linn S: Molecular mechanisms of mammalian DNA repair and the DNA damage checkpoints. Annu Rev Biochem 73: 39-85, 2004.
10. Castedo M, Perfettini JL, Roumier T, Andreau K, Medema R and Kroemer G: Cell death by mitotic catastrophe: A molecular definition. Oncogene 23: 2825-2837, 2004.
11. Vitale I, Galluzzi L, Castedo M and Kroemer G: Mitotic catastrophe: A mechanism for avoiding genomic instability. Nat Rev Mol Cell Biol 12: 385-392, 2011.
12. Meng X, Bi J, Li Y, Yang S, Zhang Y, Li M, Liu H, Li Y, McDonald ME, Thiel KW, *et al*: AZD1775 increases sensitivity to olaparib and gemcitabine in cancer cells with p53 mutations. Cancers (Basel) 10: 149, 2018.
13. Lin X, Chen D, Zhang C, Zhang X, Li Z, Dong B, Gao J and Shen L: Augmented antitumor activity by olaparib plus AZD1775 in gastric cancer through disrupting DNA damage repair pathways and DNA damage checkpoint. J Exp Clin Cancer Res 37: 129, 2018.
14. Prystowsky MB, Adomako A, Smith RV, Kawachi N, McKimpson W, Atadja P, Chen Q, Schlecht NF, Parish JL, Childs G, *et al*: The histone deacetylase inhibitor LBH589 inhibits expression of mitotic genes causing G2/M arrest and cell death in head and neck squamous cell carcinoma cell lines. J Pathol 218: 467-477, 2009.
15. Iglesias-Linares A, Yañez-Vico RM and González-Moles MA: Potential role of HDAC inhibitors in cancer therapy: Insights into oral squamous cell carcinoma. Oral Oncol 46: 323-329, 2010.
16. Lu YS, Kashida Y, Kulp SK, Wang YC, Wang D, Hung JH, Tang M, Lin ZZ, Chen TJ, Cheng AL, *et al*: Efficacy of a novel histone deacetylase inhibitor in murine models of hepatocellular carcinoma. Hepatology 46: 1119-1130, 2007.
17. Ozaki K, Kishikawa F, Tanaka M, Sakamoto T, Tanimura S and Kohno M: Histone deacetylase inhibitors enhance the chemosensitivity of tumor cells with cross-resistance to a wide range of DNA-damaging drugs. Cancer Sci 99: 376-384, 2008.
18. Ji M, Li Z, Lin Z and Chen L: Antitumor activity of the novel HDAC inhibitor CUDC-101 combined with gemcitabine in pancreatic cancer. Am J Cancer Res 8: 2402-2418, 2018.
19. Zhou L, Zhang Y, Chen S, Kmieciak M, Leng Y, Lin H, Rizzo KA, Dumur CI, Ferreira-Gonzalez A, Dai Y and Grant S: A regimen combining the Wee1 inhibitor AZD1775 with HDAC inhibitors targets human acute myeloid leukemia cells harboring various genetic mutations. Leukemia 29: 807-818, 2015.
20. Qi W, Zhang W, Edwards H, Chu R, Madlambayan GJ, Taub JW, Wang Z, Wang Y, Li C, Lin H and Ge Y: Synergistic anti-leukemic interactions between panobinostat and MK-1775 in acute myeloid leukemia ex vivo. Cancer Biol Ther 16: 1784-1793, 2015.
21. Tanaka N, Patel AA, Tang L, Silver NL, Lindemann A, Takahashi H, Jaksik R, Rao X, Kalu NN, Chen TC, *et al*: Replication stress leading to apoptosis within the S-phase contributes to synergism between vorinostat and AZD1775 in HNSCC harboring high-risk TP53 mutation. Clin Cancer Res 23: 6541-6554, 2017.
22. Hattori K, Takano N, Kazama H, Moriya S, Miyake K, Hiramoto M, Tsukahara K and Miyazawa K: Synergistic non-apoptotic cell death induction by simultaneously targeting proteasome with bortezomib and HDAC6 with ricolinostat in head and neck tumor cells. Oncol Lett 22: 680, 2021.
23. Wickström SA, Masoumi KC, Khochbin S, Fässler R and Massoumi R: CYLD negatively regulates cell-cycle progression by inactivating HDAC6 and increasing the levels of acetylated tubulin. Embo J 29: 131-144, 2010.
24. Kim IA, No M, Lee JM, Shin JH, Oh JS, Choi EJ, Kim IH, Atadja P and Bernhard EJ: Epigenetic modulation of radiation response in human cancer cells with activated EGFR or HER-2 signaling: Potential role of histone deacetylase 6. Radiother Oncol 92: 125-132, 2009.
25. Namdar M, Perez G, Ngo L and Marks PA: Selective inhibition of histone deacetylase 6 (HDAC6) induces DNA damage and sensitizes transformed cells to anticancer agents. Proc Natl Acad Sci USA 107: 20003-20008, 2010.
26. Wang L, Xiang S, Williams KA, Dong H, Bai W, Nicosia SV, Khochbin S, Bepler G and Zhang X: Depletion of HDAC6 enhances cisplatin-induced DNA damage and apoptosis in non-small cell lung cancer cells. PLoS One 7: e44265, 2012.
27. Toriyama K, Takano N, Kokuba H, Kazama H, Moriya S, Hiramoto M, Abe S and Miyazawa K: Azithromycin enhances the cytotoxicity of DNA-damaging drugs via lysosomal membrane permeabilization in lung cancer cells. Cancer Sci 112: 3324-3337, 2021.
28. Pemble H, Kumar P, van Haren J and Wittmann T: GSK3-mediated CLASP2 phosphorylation modulates kinetochore dynamics. J Cell Sci 130: 1404-1412, 2017.
29. Spangle JM, Ghosh-Choudhury N and Munger K: Activation of cap-dependent translation by mucosal human papillomavirus E6 proteins is dependent on the integrity of the LXXLL binding motif. J Virol 86: 7466-7472, 2012.
30. Szalai P and Engedal N: An image-based assay for high-throughput analysis of cell proliferation and cell death of adherent cells. Bio-protocol 8: e2835, 2018.
31. Vakifahmetoglu H, Olsson M and Zhivotovsky B: Death through a tragedy: Mitotic catastrophe. Cell Death Differ 15: 1153-1162, 2008.
32. Ghelli Luserna di Rorà A, Cerchione C, Martinelli G and Simonetti G: A WEE1 family business: Regulation of mitosis, cancer progression, and therapeutic target. J Hematol Oncol 13: 126, 2020.
33. Santo L, Hideshima T, Kung AL, Tseng JC, Tamang D, Yang M, Jarpe M, van Duzer JH, Mazitschek R, Ogier WC, *et al*: Preclinical activity, pharmacodynamic, and pharmacokinetic properties of a selective HDAC6 inhibitor, ACY-1215, in combination with bortezomib in multiple myeloma. Blood 119: 2579-2589, 2012.
34. Chen X, Low KH, Alexander A, Jiang Y, Karakas C, Hess KR, Carey JP, Bui TN, Vijayaraghavan S, Evans KW, *et al*: Cyclin E overexpression sensitizes triple-negative breast cancer to Wee1 kinase inhibition. Clin Cancer Res 24: 6594-6610, 2018.
35. Young LA, O'Connor LO, de Renty C, Veldman-Jones MH, Dorval T, Wilson Z, Jones DR, Lawson D, Odedra R, Maya-Mendoza A, *et al*: Differential activity of ATR and WEE1 inhibitors in a highly sensitive subpopulation of DLBCL linked to replication stress. Cancer Res 79: 3762-3775, 2019.
36. Do K, Doroshow JH and Kummar S: Wee1 kinase as a target for cancer therapy. Cell Cycle 12: 3159-3164, 2013.
37. Cuneo KC, Morgan MA, Sahai V, Schipper MJ, Parsels LA, Parsels JD, Devasia T, Al-Hawaray M, Cho CS, Nathan H, *et al*: Dose escalation trial of the Wee1 inhibitor Adavosertib (AZD1775) in combination with gemcitabine and radiation for patients with locally advanced pancreatic cancer. J Clin Oncol 37: 2643-2650, 2019.
38. Leijen S, van Geel RM, Sonke GS, de Jong D, Rosenberg EH, Marchetti S, Pluim D, van Werkhoven E, Rose S, Lee MA, *et al*: Phase II study of WEE1 inhibitor AZD1775 plus carboplatin in patients with TP53-mutated ovarian cancer refractory or resistant to first-line therapy within 3 months. J Clin Oncol 34: 4354-4361, 2016.
39. Lheureux S, Cabanero M, Cristea MC, Mantia-Smaldone G, Olawaiye A, Ellard S, Weberpals JI, Hendrickson AEW, Fleming GF, Welch S, *et al*: A randomized double-blind placebo-controlled phase II trial comparing gemcitabine monotherapy to gemcitabine in combination with adavosertib in women with recurrent, platinum resistant epithelial ovarian cancer: A trial of the Princess Margaret, California, Chicago and Mayo Phase II Consortia. J Clin Oncol 37: 5518-5518, 2019.
40. Oza AM, Estevez-Diz M, Grischke EM, Hall M, Marmé F, Provencher D, Uyar D, Weberpals JI, Wenham RM, Laing N, *et al*: A Biomarker-enriched, randomized phase II trial of adavosertib (AZD1775) plus paclitaxel and carboplatin for women with platinum-sensitive TP53-mutant ovarian cancer. Clin Cancer Res 26: 4767-4776, 2020.
41. Liu JF, Xiong N, Campos SM, Wright AA, Krasner C, Schumer S, Horowitz N, Veneris J, Tayob N, Morrissey S, *et al*: Phase II study of the WEE1 inhibitor adavosertib in recurrent uterine serous carcinoma. J Clin Oncol 39: 1531-1539, 2021.

42. Ku BM, Bae YH, Koh J, Sun JM, Lee SH, Ahn JS, Park K and Ahn MJ: Mutational status of *TP53* defines the efficacy of Wee1 inhibitor AZD1775 in *KRAS*-mutant non-small cell lung cancer. Oncotarget 8: 67526-67537, 2017.
43. Kreahling JM, Foroutan P, Reed D, Martinez G, Razabdouski T, Bui MM, Raghavan M, Letson D, Gillies RJ and Altiok S: Wee1 inhibition by MK-1775 leads to tumor inhibition and enhances efficacy of gemcitabine in human sarcomas. PLoS One 8: e57523, 2013 (Epub ahead of print).
44. Moses N, Zhang M, Wu JY, Hu C, Xiang S, Geng X, Chen Y, Bai W, Zhang YW, Bepler G and Zhang XM: HDAC6 regulates radiosensitivity of non-small cell lung cancer by promoting degradation of Chk1. Cells 9: 2237, 2020.
45. Hubbert C, Guardiola A, Shao R, Kawaguchi Y, Ito A, Nixon A, Yoshida M, Wang XF and Yao TP: HDAC6 is a microtubule-associated deacetylase. Nature 417: 455-458, 2002.
46. Kovacs JJ, Murphy PJ, Gaillard S, Zhao X, Wu JT, Nicchitta CV, Yoshida M, Toft DO, Pratt WB and Yao TP: HDAC6 regulates Hsp90 acetylation and chaperone-dependent activation of glucocorticoid receptor. Mol Cell 18: 601-607, 2005.
47. Zhang X, Yuan Z, Zhang Y, Yong S, Salas-Burgos A, Koomen J, Olashaw N, Parsons JT, Yang XJ, Dent SR, *et al*: HDAC6 modulates cell motility by altering the acetylation level of cortactin. Mol Cell 27: 197-213, 2007.
48. Lee YS, Lim KH, Guo X, Kawaguchi Y, Gao Y, Barrientos T, Ordentlich P, Wang XF, Counter CM and Yao TP: The cytoplasmic deacetylase HDAC6 is required for efficient oncogenic tumorigenesis. Cancer Res 68: 7561-7569, 2008.
49. Lernoux M, Schnekenburger M, Dicato M and Diederich M: Anti-cancer effects of naturally derived compounds targeting histone deacetylase 6-related pathways. Pharmacol Res 129: 337-356, 2018.
50. Bradbury CA, Khanim FL, Hayden R, Bunce CM, White DA, Drayson MT, Craddock C and Turner BM: Histone deacetylases in acute myeloid leukaemia show a distinctive pattern of expression that changes selectively in response to deacetylase inhibitors. Leukemia 19: 1751-1759, 2005.
51. Sakuma T, Uzawa K, Onda T, Shiiba M, Yokoe H, Shibahara T and Tanzawa H: Aberrant expression of histone deacetylase 6 in oral squamous cell carcinoma. Int J Oncol 29: 117-124, 2006.
52. Bazzaro M, Lin Z, Santillan A, Lee MK, Wang MC, Chan KC, Bristow RE, Mazitschek R, Bradner J and Roden RB: Ubiquitin proteasome system stress underlies synergistic killing of ovarian cancer cells by bortezomib and a novel HDAC6 inhibitor. Clin Cancer Res 14: 7340-7347, 2008.
53. Cao J, Lv W, Wang L, Xu J, Yuan P, Huang S, He Z and Hu J: Ricolinostat (ACY-1215) suppresses proliferation and promotes apoptosis in esophageal squamous cell carcinoma via miR-30d/PI3K/AKT/mTOR and ERK pathways. Cell Death Dis 9: 817, 2018.
54. Kanno K, Kanno S, Nitta H, Uesugi N, Sugai T, Masuda T, Wakabayashi G and Maesawa C: Overexpression of histone deacetylase 6 contributes to accelerated migration and invasion activity of hepatocellular carcinoma cells. Oncol Rep 28: 867-873, 2012.
55. Chuang MJ, Wu ST, Tang SH, Lai XM, Lai HC, Hsu KH, Sun KH, Sun GH, Chang SY, Yu DS, *et al*: The HDAC inhibitor LBH589 induces ERK-dependent prometaphase arrest in prostate cancer via HDAC6 inactivation and down-regulation. PLoS One 8: e73401, 2013.
56. Vicente JJ and Wordeman L: The quantification and regulation of microtubule dynamics in the mitotic spindle. Curr Opin Cell Biol 60: 36-43, 2019.
57. Ling L, Hu F, Ying X, Ge J and Wang Q: HDAC6 inhibition disrupts maturational progression and meiotic apparatus assembly in mouse oocytes. Cell Cycle 17: 550-556, 2018.